Inherent structures in models for fragile and strong glass

Luca Leuzzi and Theo M. Nieuwenhuizen
Universiteit van Amsterdam, Valckenierstraat 65, 1018 XE Amsterdam, The Netherlands
(Received 8 March 2001; published 26 November 2001)

An analysis of the dynamics is performed of exactly solvable models for fragile and strong glasses, exploiting the partitioning of the free-energy landscape in inherent structures. The results are compared with the exact solution of the dynamics, by employing the formulation of an effective temperature used in literature. Also, a statistical mechanics formulation is introduced, based upon general statistical considerations, which performs better. Though the considered models are conceptually simple, there is no limit in which the dynamics may be exactly described by a symbolic dynamics of the system moving through consistently weighted inherent structures.

DOI: 10.1103/PhysRevE.64.066125 PACS number(s): 05.70.Ln, 61.43.Fs, 61.20.Lc, 05.10.Ln

I. INTRODUCTION

The characteristics of a glassy system [1,2] arise from the complex topography of the multidimensional function representing the collective potential energy that gives rise to a nontrivial partition function and thermodynamic potential. In this picture, at low enough temperature where vibrations are minimal, the spatial atomic patterns in crystals and in amorphous systems share the common basic attribute that both represent minima in the potential-energy function describing the interactions. The presence of distinct processes acting on two different time scales means that the deep and wide local minima at and below the glass transition temperature T_g are geometrically organized to create a two length-scale potential-energy pattern. T_g depends on the cooling procedure and it is usually determined as the temperature at which the viscosity of the glass former reaches the value of 10^{13}.

In the present paper, we investigate, using the inherent structure approach, exactly solvable model glass that shows all the basic features of real glasses [3]. We study two models: one for the fragile glass and one for the strong one. The models are built by processes evolving on two different, well-separated time scales, representing, respectively, the α and β processes taking place in real glassy materials. The slow α processes represent the escape from one deep minimum within a large scale valley to another valley. The fast β processes, instead, are related to elementary relaxations between neighboring minima inside the same valley. We consider here all kinds of β processes as equivalent, since the characteristic time scales on which they are evolving are in any case much shorter than the time scale of the α processes (i.e., the observation time).

In the general case, decreasing the temperature, the free-energy local minima may, in principle, be split into smaller local minima. But if we may assume that they maintain their identity in spite of this splitting, we can set a one-to-one correspondence between local minima and inherent structures [4–7], i.e., between the minima of the free energy and the ones of the potential energy. Actually, such a splitting does not even occur in the two dynamical models presented here, making the correspondence exact at all temperatures. The same happens, for instance, in mean-field spin-glass models, such as *p*-spinlike models [8–11].

In this paper, we will see to which extent such a scheme, widely used in numerical simulations [4–6,8–10,12,13], applies to our analytically solvable models. We will compare it with the exact dynamic solution, achieved without any partitioning of the configuration space.

In Sec. II, we introduce the two kinetic models and we give the description of their statics and of their Monte Carlo dynamics. In Sec. III, we develop the inherent structure approach for the dynamics of such models and we define two different inherent structure-effective temperatures mapping the dynamics into a thermodynamic frame (in Sec. III D); one definition follows the literature on numerical simulations [4–10,12,13], the other exploits the analytic solvability of the models.

II. THE MODELS AND THEIR PROPERTIES

A. Hamiltonian and constraint on the configuration space

We present two dynamical models, having the same statics, but different dynamics leading to the behavior of a fragile glass in one case and to the behavior of a strong glass in the other one. The model describing a system relaxing like a fragile glass was introduced in [15] and widely studied in [3].

Both models are described by the following local Hamiltonian:

$$\mathcal{H}[\{x_i\},\{S_i\}]=\frac{1}{2}K\sum_{i=1}^{N}x_i^2-H\sum_{i=1}^{N}x_i-J\sum_{i=1}^{N}x_iS_i-L\sum_{i=1}^{N}S_i, \tag{2.1}$$

where N is the size of the system and $\{x_i\}$ and $\{S_i\}$ are continuous variables, the last satisfying a spherical constraint: $\Sigma_i S_i^2=N$. We call them, respectively, harmonic oscillators and spherical spins. K is the Hooke elastic constant, H is an external field acting on the harmonic oscillators, J is the coupling constant between $\{x_i\}$ and $\{S_i\}$ on the same site i, and L is the external field acting on the spherical spins. A separation of time scales is introduced by hand: the spins represent the fast modes and the harmonic oscillators the slow ones. We assume that the $\{S_i\}$ relax to equilibrium on a time scale much shorter than the one of the harmonic oscillators. From the point of view of the motion of the $\{x_i\}$, the

spins are just a noise. To describe the long-time regime of the $\{x_i\}$, in [3], we can average over this noise by performing the computation of the $\{S_i\}$ partition function, obtaining an effective Hamiltonian depending only on the $\{x_i\}$, that determines the dynamics of these variables [in the analysis with inherent structures, we will not carry out this average but we will start from the ''bare'' Hamiltonian, Eq. (2.1)]. Using the saddle-point approximation for large N we find,

$$\begin{aligned} Z_S(\{x_i\}) &= \int \left(\prod_{i=1}^{N} dS_i \right) \exp\{-\beta \mathcal{H}[\{x_i\},\{S_i\}]\} \\ &\quad \times \delta\left(\sum_{i=1}^{N} S_i^2 - N \right) \\ &\simeq \exp\left[-\beta N \left(\frac{K}{2} m_2 - H m_1 - w + \frac{T}{2} \ln \frac{w + T/2}{T} \right) \right], \end{aligned} \tag{2.2}$$

where we introduce the short hands

$$m_1 \equiv \frac{1}{N} \sum_{i=1}^{N} x_i, \quad m_2 \equiv \frac{1}{N} \sum_{i=1}^{N} x_i^2, \tag{2.3}$$

and

$$w \equiv \sqrt{J^2 m_2 + 2JL m_1 + L^2 + \frac{T^2}{4}}. \tag{2.4}$$

We define, then, the effective Hamiltonian $\mathcal{H}_{\text{eff}}(\{x_i\}) \equiv -T \ln Z_S(\{x_i\})$, that is the free energy for a given configuration of $\{x_i\}$. We find

$$\mathcal{H}_{\text{eff}}(\{x_i\}) = \frac{K}{2} m_2 N - H m_1 N - wN + \frac{TN}{2} \ln \frac{w + T/2}{T}. \tag{2.5}$$

This may also be written in terms of the internal energy $U(\{x_i\})$ and of the entropy $S_{\text{ep}}(\{x_i\})$ of the equilibrium processes (i.e., the spins),

$$\mathcal{H}_{\text{eff}}(\{x_i\}) = U(\{x_i\}) - T S_{\text{ep}}(\{x_i\}), \tag{2.6}$$

$$U(\{x_i\}) = \frac{K}{2} m_2 N - H m_1 N - wN + \frac{TN}{2}, \tag{2.7}$$

$$S_{\text{ep}}(\{x_i\}) = \frac{N}{2} - \frac{N}{2} \ln \frac{w + T/2}{T}. \tag{2.8}$$

The function U is actually the Hamiltonian averaged over the spins and S_{ep} is the entropy of the spins.

In [3], we studied the model characterized by a constraint on the phase space, introduced for the fragile glass case to avoid the existence of the single-global minimum, and implementing a large degeneracy of the allowable lowest states. The constraint is taken on the $\{x_i\}$, thus concerning the long time regime. It reads

$$m_2 - m_1^2 \geqslant m_0, \tag{2.9}$$

where m_0 is a model parameter. It is a fixed, but arbitrary, strictly positive constant. This constraint applied to the harmonic-oscillators dynamics is a way to reproduce the behavior of good glass formers. We imposed a Monte Carlo dynamics [16,17] satisfying this constraint and coupling the otherwise noninteracting $\{x_i\}$ in a dynamic way. As we saw in [3], the system exhibits a Vogel-Fulcher-Tammann-Hesse (VFTH) relaxation [24], characterizing a fragile glass.

To model a strong glass, instead, we will consider the same model Hamiltonian but without imposing any constraint and making use of a different Monte Carlo dynamics. We will show later (Appendix) that this dynamics displays an Arrhenius relaxation near zero temperature. In this case, we have a strong glass, as it happens for similar models, e.g., the oscillators model [17] and the spherical spins model [18] where exactly the same dynamics is applied. The point of the present paper is that now there are both fast and slow processes.

To shorten the notation, we define the modified ''spring constant'' $\tilde{K}$ and ''external field'' $\tilde{H}$,

$$\tilde{K} = K - \frac{J^2}{w + T/2}, \quad \tilde{H} = H + \frac{JL}{w + T/2}. \tag{2.10}$$

We stress that $\tilde{K}$ and $\tilde{H}$ are actually functions of the $\{x_i\}$ themselves (through m_1 and m_2, occurring in w). We also define the constant

$$D \equiv HJ + KL. \tag{2.11}$$

Using the definitions (2.10) it is useful to note that

$$\tilde{H}J + \tilde{K}L = HJ + KL = D. \tag{2.12}$$

B. Statics at heat-bath temperature T

The partition function of the whole system at equilibrium is

$$\begin{aligned} Z(T) &= \int \mathcal{D}x \mathcal{D}S \exp[-\beta \mathcal{H}(\{x_i\},\{S_i\})] \delta\left(\sum_i x_i^2 - N \right) \\ &= \int dm_1\, dm_2 \exp\left\{ -\beta N \left[\frac{K}{2} m_2 - H m_1 - w \right.\right. \\ &\quad \left.\left. + \frac{T}{2} \ln\left(\frac{w + T/2}{T} \right) - \frac{T}{2} [1 + \ln(m_2 - m_1^2)] \right] \right\}. \end{aligned} \tag{2.13}$$

The new object that appears in the exponent is the configurational entropy

$$\mathcal{I} \equiv \frac{N}{2} [1 + \ln(m_2 - m_1^2)]. \tag{2.14}$$

It comes from the Jacobian $\exp\{\mathcal{I}\}$ of the transformation of variables $\mathcal{D}x \to dm_1\, dm_2$ [see Eq. (2.3)]. We may compute the large N limit of this partition function using, once again, the saddle-point approximation. The saddle-point equations are found minimizing the expression between square brackets in Eq. (2.13) with respect to m_1 and m_2. This yields

$$\bar{m}_1 = \frac{\tilde{H}(\bar{m}_1, \bar{m}_2)}{\tilde{K}(\bar{m}_1, \bar{m}_2)}, \tag{2.15}$$

$$\bar{m}_2 = \bar{m}_1^2 + \frac{T}{\tilde{K}(\bar{m}_1, \bar{m}_2)}. \tag{2.16}$$

The form of the solutions $\bar{m}_1(T)$, $\bar{m}_2(T)$ is quite complicated because each of these equations is actually a fourth-order equation, but they can be explicitly computed. In terms of the equilibrium values $\bar{m}_k$, we find the following expression for the equilibrium free energy:

$$F[T, \bar{m}_1(T), \bar{m}_2(T)] = N\left\{ \frac{K}{2}\bar{m}_2 - H\bar{m}_1 - w(\bar{m}_1, \bar{m}_2) + \frac{T}{2}\left[\ln \frac{w(\bar{m}_1, \bar{m}_2) + T/2}{T} - [1 + \ln(\bar{m}_2 - \bar{m}_1^2)] \right] \right\} \tag{2.17}$$

$$= U(T, \bar{m}_1, \bar{m}_2) - TS_{\mathrm{ep}}(T, \bar{m}_1, \bar{m}_2) - T\mathcal{I}(T, \bar{m}_1, \bar{m}_2). \tag{2.18}$$

This is the statics both for the model with the constraint (2.9), as long as the temperature exceeds the Kauzmann temperature, and for the one without it. Indeed, for the fragile glass case at $T \leqslant T_0$, when the constraint is reached, the saddle-point Eq. (2.16) becomes $\bar{m}_2 - \bar{m}_1^2 = m_0$, no matter what the temperature is of the thermal bath. In this paper, however, we will limit ourselves, for the fragile glass, to cases where T is larger than T_0.

C. Dynamics

The dynamics we apply to the system is a parallel Monte Carlo dynamics, first introduced in [16]. The thus obtained dynamical model composed by the simple local Hamiltonian (2.1) and such a dynamics has the benefit of being analytically solvable.

In a Monte Carlo step, a random updating of the variables is performed ($x_i \to x_i' = x_i + r_i/\sqrt{N}$) where the $\{r_i\}$ have a Gaussian distribution with zero mean and variance Δ^2. We define $x \equiv \mathcal{H}(\{x_i'\}) - \mathcal{H}(\{x_i\})$ as the energy difference between the new and the old state. If $x > 0$, the move is accepted with a probability $W(\beta x) \equiv \exp(-\beta x)$; else it is always accepted [$W(\beta x) = 1$]. The updating is made in parallel. It is the parallel nature of the updating that allows the collective behavior leading to exponentially divergent time scales in models with no interactions between particles such us ours. A sequential updating would not produce any glassy effect. This dynamics may induce glassy behavior in situations where ordinary Glauber dynamics [19] would not. In our paper, the parallel dynamics mimics the presence of interactions between atoms in realistic glasses, where a large internal cooperativeness is present. For different examples of dynamics implying nontrivial collective behavior, the reader may look, for instance, at the n spin facilitated kinetic Ising model [20,21] or at the kinetic lattice-gas model [22,23].

In a Monte Carlo step, the quantities $\Sigma_i x_i = N m_1$ and $\Sigma_i x_i^2 = N m_2$ are updated. We denote their change by y_1 and y_2, respectively. Their distribution function is, for given values of m_1 and m_2,

$$p(y_1, y_2 | m_1, m_2) \equiv \int \prod_i \frac{dr_i e^{-r_i^2/(2\Delta^2)}}{\sqrt{2\pi\Delta^2}} \delta\left(\sum_i x_i' - \sum_i x_i - y_1 \right) \times \delta\left(\sum_i x'^2_i - \sum_i x_i^2 - y_2 \right)$$

$$= \frac{1}{4\pi\Delta^2\sqrt{m_2 - m_1^2}} \times \exp\left(-\frac{y_1^2}{2\Delta^2} - \frac{(y_2 - \Delta^2 - 2y_1 m_1)^2}{8\Delta^2(m_2 - m_1^2)} \right). \tag{2.19}$$

Neglecting the variations of m_1 and m_2 of order Δ^2/N, we may express the energy difference as [3]

$$x = \frac{\tilde{K}}{2} y_2 - \tilde{H} y_1. \tag{2.20}$$

In terms of x and $y = y_1$, the distribution function may be formally written as the product of two Gaussian distributions

$$p(y_1, y_2 | m_1, m_2)\, dy_1\, dy_2 = dx\, p(x | m_1, m_2)\, dy\, p(y | x, m_1, m_2) = \frac{dx}{\sqrt{2\pi\Delta_x}} \exp\left(-\frac{(x - \bar{x})^2}{2\Delta_x} \right) \times \frac{dy}{\sqrt{2\pi\Delta_y}} \exp\left(-\frac{[y - \bar{y}(x)]^2}{2\Delta_y} \right), \tag{2.21}$$

where

$$\bar{x} = \Delta^2\tilde{K}/2, \quad \Delta_x = \Delta^2\tilde{K}^2(m_2 - m_1^2) + \Delta^2\tilde{K}^2(m_1 - \tilde{H}/\tilde{K})^2, \tag{2.22}$$

$$\bar{y}(x) = \frac{m_1 - \tilde{H}/\tilde{K}}{m_2 - m_1^2 + (m_1 - \tilde{H}/\tilde{K})^2} \frac{x - \bar{x}}{\tilde{K}},$$

$$\Delta_y = \frac{\Delta^2(m_2 - m_1^2)}{m_2 - m_1^2 + (m_1 - \tilde{H}/\tilde{K})^2}. \tag{2.23}$$

1. Dynamics of the fragile glass model

To represent a fragile glass, the dynamics that we apply to the system is a generalization of the analytic treatment of Monte Carlo dynamics introduced in [16]. As noted in [15], also in this generalized case, the dynamical model with a contrived dynamics may be analytically solved. As we saw in [3], in the long-time domain, the dynamics looks quite reasonable with regard to what one might expect of any glassy system and the system exhibits a VFTH relaxation. We repeat here the main steps of the implementation of this dynamics (for a more extended presentation see [3]).

We let Δ^2, the variance of the random updating $\{r_i\}$, depend on the distance from the constraint, i.e., on the whole $\{x_i\}$ configuration before the Monte Carlo update

$$\Delta^2(t) \equiv 8[m_2(t) - m_1^2(t)] \left(\frac{B}{m_2(t) - m_1^2(t) - m_0} \right)^{\gamma}, \tag{2.24}$$

where B, m_0, and γ are constants. In particular, γ is an exponent larger than zero that appears in the VFTH-like relaxation law of the model, when T decreases towards some critical temperature T_0 (in [3], we showed that T_0 is the Kauzmann temperature of the model)

$$\tau_{\mathrm{eq}} \sim \exp\left(\frac{A_{\mathrm{f}}}{T - T_0} \right)^{\gamma}. \tag{2.25}$$

A_{f} is a constant depending on the system's parameters. In other models [16–18,25,26] the variance Δ^2 was kept constant. We will keep it constant in the dynamics of our strong glass model as well (see next section).

For what concerns the VFTH exponent γ we saw in [3] that it generates different dynamic regimes for $\gamma > 1$, $\gamma = 1$, and $0 < \gamma < 1$; the situation $\gamma = 1$ remains model dependent even in the long-time limit. We will stay in the following in the regime for $\gamma > 1$.

The nearer the system goes to the constraint (i.e., the smaller the value of $m_2 - m_1^2 - m_0$), the larger the variance Δ^2, implying almost always a refusal of the proposed updating. In this way, in the neighborhood of the constraint, the dynamics is very slow and goes on through very seldom but very large moves, which may be interpreted as activated processes. When the constraint is reached, the variance Δ^2 becomes infinite and the system dynamics gets stuck. The system does not evolve anymore towards equilibrium but it is blocked in one single ergodic component of the configuration space. At large enough temperatures, the combination $m_2(t) - m_1^2(t) - m_0$ will remain strictly positive. The highest temperature, T_0, at which it can vanish for $t \to \infty$, is identified with the Kauzmann temperature [3].

The dynamics may be expressed in terms of two combinations of m_1 and m_2. The first one, defined as

$$\mu_1 \equiv \frac{\widetilde{H}}{\widetilde{K}} - m_1, \tag{2.26}$$

represents the distance from the instantaneous equilibrium state. By instantaneous equilibrium state, we mean that $\widetilde{H}$ and $\widetilde{K}$ depend on the values of m_1 and m_2 at a given time t. For $t \to \infty$, at the true equilibrium, one has $\mu_1 = 0$.

The second dynamical variable is defined as the distance from the constraint (2.9)

$$\mu_2 \equiv m_2 - m_1^2 - m_0. \tag{2.27}$$

When $\mu_2 = 0$, the constraint is reached. This will happen if the temperature is low enough ($T \leqslant T_0$) and the time large enough. T_0 is the highest temperature at which the constraint is asymptotically ($t \to \infty$) reached by the system. Above T_0, ordinary equilibrium will be achieved without reaching the constraint. The temperature is, then, too high for the system to notice that there is a constraint at all on the configurations (we are speaking about the asymptotic time regime), and this implies [see Eq. (2.16)]

$$\lim_{t \to \infty} \mu_2(t) = \overline{\mu}_2(T) = \frac{T}{\widetilde{K}_\infty(T)} - m_0 > 0, \tag{2.28}$$

where

$$\widetilde{K}_\infty(T) \equiv \lim_{t \to \infty} \widetilde{K}[m_1(t), m_2(t); T] = \widetilde{K}[\overline{m}_1(T), \overline{m}_2(T)]. \tag{2.29}$$

Below T_0, the system goes to configurations that become arbitrarily close to the constraint, and then stay there arbitrarily long. Note that, by definition of T_0, we may write

$$m_0 = \frac{T_0}{\widetilde{K}_\infty(T_0)}. \tag{2.30}$$

Solving the equations of motions, for fixed parameters (aging setup), we find, to the leading orders of approximation for large times, the following behavior for μ_2 [3]

$$\mu_2(t) \simeq \frac{B}{\{\ln(t/t_0) + c \ln[\ln(t/t_0)]\}^{1/\gamma}}, \tag{2.31}$$

where $c = 1/2$ since, in this paper, we only look at the regime for $T \geqslant T_0$. The constant t_0 depends on the parameters of the model and on the temperature; it is of order one. The solution (2.31) is valid in the aging regime, where $t_0 \ll t \ll \tau_{eq}(T)$. Indeed, when $t \sim \tau_{eq}(T) \sim \exp[A/(T - T_0)]^{\gamma}$ the "distance" μ_2 becomes

$$\mu_2 \simeq \frac{B}{\left[\left(\frac{A_{\mathrm{f}}}{T - T_0} \right)^{1/\gamma} \right]^{\gamma}} \propto T - T_0, \tag{2.32}$$

as it should be.

We also introduce another variable that will be useful later on, namely, the difference between $\mu_2(t)$ and its asymptotic, equilibrium, value $\overline{\mu}_2(T)$

$$\delta\mu_2(t)\equiv\mu_2(t)-\overline{\mu}_2(T)\simeq\frac{B}{\{\log(t/t_0)+c\,\ln[\log(t/t_0)]\}^{1/\gamma}}-\frac{T}{\tilde{K}_\infty(T)}+\frac{T_0}{\tilde{K}_\infty(T_0)},\tag{2.33}$$

where, using Eq. (2.30), $\overline{\mu}_2(T)$ comes from Eq. (2.28), valid, in the fragile case, when $T\geqslant T_0$. When $t\to\infty$, $\delta\mu_2=0$, by definition.

The dynamical behavior of μ_1 depends not only on the temperature (above or below T_0) but also on γ being greater, equal to, or less than one. With respect to the relative weight of μ_1 and μ_2, we may identify different regimes [3]. What is of our interest here is the regime of $T\geqslant T_0$ and $\gamma>1$, where $\mu_1(t)\ll\mu_2(t)$ and a unique effective thermodynamic parameter may be properly defined in various independent ways [3].

2. Dynamics of the strong glass model

We now analyze the simple case without constraint on the configuration space and with a constant Δ^2, the variance of the randomly chosen updating $\{r_i\}$ of the slow variables $\{x_i\}$. This dynamical model may also be seen as the limit for $m_0\to0$ and $\gamma\to1$ of the preceding one. We also mention that the case with $J=L=0$ is the model of harmonic oscillators studied in [17,25].

In the fragile glass case, we studied a different version of such a dynamics for two particular combinations of the variables m_1 and m_2. Here, we will keep the same notation. The first variable is thus defined, starting from the saddle-point Eq. (2.15), as the deviation from the instantaneous equilibrium state and is formally equivalent to Eq. (2.26).

The second variable is defined as

$$\mu_2\equiv m_2-m_1^2.\tag{2.34}$$

When $T=0$ from Eq. (2.16) we know that $\mu_2=0$. Indeed, at $T=0$, the system reaches its minimum

$$x_i=\frac{H+J}{K}\quad\forall i.\tag{2.35}$$

For simplicity, we limit ourselves to a choice of the interaction parameters such that $D=HJ+KL>0$ and $\tilde{K}>0$, for which this is the global minimum. In the Appendix we derive the equations of motion for μ_1 and μ_2 and we solve them for temperature equal to and slightly above zero and long times, in the aging regime. In this time regime, μ_1 turns out to be much smaller than μ_2: $\mu_1\propto\mu_2^2$. The solution for μ_2 is, at the leading order

$$\mu_2(t)\simeq\frac{\Delta^2}{8}\frac{1}{\ln\frac{2t}{\sqrt{\pi}}}.\tag{2.36}$$

The difference $\delta\mu_2(t)$, between $\mu_2(t)$ and its asymptotic value, is now

$$\delta\mu_2(t)\equiv\mu_2(t)-\overline{\mu}_2(T)\simeq\frac{\Delta^2}{8}\frac{1}{\ln\frac{2t}{\sqrt{\pi}}}-\frac{T}{\tilde{K}_\infty(T)},\tag{2.37}$$

where $\overline{\mu}_2(T)$ comes from Eq. (2.16) and

$$\tilde{K}_\infty(T)=\lim_{t\to\infty}\tilde{K}(m_1(t),m_2(t);T)=\frac{KD}{D+J^2}+\frac{T}{2}\frac{J^2K^2}{(D+J^2)^2}+\frac{T^2}{8}\frac{J^6K^3(J^2-3D)}{D(D+J^2)^5}+O(T^3),\tag{2.38}$$

for $t\to\infty$, $\delta\mu_2(t)\to0$.

At low temperature, the relaxation time for the slow processes follows an Arrhenius law

$$\tau_{\rm eq}(T)\propto\exp\left(\frac{A_{\rm s}}{T}\right),\tag{2.39}$$

with

$$A_{\rm s}\equiv\frac{\Delta^2\tilde{K}_\infty(0)}{8}.\tag{2.40}$$

D. Two temperature thermodynamics

Before going on, we recall here that we are able to introduce effective parameters in order to rephrase the dynamics of the system out of equilibrium into a thermodynamic description (for a review, see [25]).

In [3], we got through different methods the following expression for the effective temperature in the regime for $T>T_0$ as a function of the interaction parameters of the model and of the time evolution of its observables

$$T_e(t)=\tilde{K}[m_1(t),m_2(t)][m_0+\mu_2(t)].\tag{2.41}$$

Since we will use one of these methods in the next section to map the inherent structure (IS) dynamics into an effective thermodynamic parameter, we shortly recall this particular derivation of Eq. (2.41). Knowing the solution of the dynamics at a given time t, a quasistatic approach may be followed by computing the partition function Z_e of all the macroscopically equivalent states at the time t. In order to generalize the equilibrium thermodynamics, we assume an effective temperature T_e and an effective field H_e, and substitute the Boltzmann-Gibbs equilibrium measure by $\exp[-\mathcal{H}_{\rm eff}(\{x_i\},T,H_e)/T_e]$, where $\mathcal{H}_{\rm eff}$ is given in Eq. (2.6) and the true external field H has been substituted by the effective field H_e. As we get the expression of the "thermodynamic" potential $F_e\equiv-T_e\log Z_e$ as a function of macroscopic variables $m_{1,2}$ and effective parameters, we may determine T_e and H_e minimizing F_e with respect to m_1 and m_2 and evaluating the resulting analytic expressions at $m_{1,2}=m_{1,2}(t)$.

The partition function of the macroscopically equivalent states is

$$Z_e(m_1,m_2;T_e,H_e) \equiv \int \mathcal{D}x \exp\left[-\frac{1}{T_e}\mathcal{H}_{\rm eff}(\{x_i\},T,H_e)\right] \times \delta\left(Nm_1-\sum_i x_i\right)\delta\left(Nm_2-\sum_i x_i^2\right). \tag{2.42}$$

From this we build the effective thermodynamic potential as a function of T_e and H_e, besides of T and H, where the effective parameters depend on time through the time-dependent values of m_1 and m_2, solutions of the dynamics. T_e and H_e are actually a way of describing the evolution in time of the system out of equilibrium. The free-energy $F_e = -T_e \log Z_e$ is minimized with respect to m_1 and m_2. Then their time-dependent values are inserted, yielding

$$F_e(t) = U[m_1(t),m_2(t)] - TS_{ep}[m_1(t),m_2(t)] - T_e(t)\mathcal{I}[m_1(t),m_2(t)] + [H-H_e(t)]Nm_1(t), \tag{2.43}$$

with

$$T_e(t) = \tilde{K}[m_1(t),m_2(t)][m_0+\mu_2(t)],$$
$$H_e(t) = H - \tilde{K}[m_1(t),m_2(t)]\mu_1(t). \tag{2.44}$$

U is the internal energy of the whole system [see Eq. (2.7)], S_{ep} is the entropy of the fast or equilibrium processes (the spherical spins) [see Eq. (2.8)] while $\mathcal{I}$ is the entropy of the slow, ''configurational,'' processes (the harmonic oscillators) [see Eq. (2.14)]. The last term of F_e replaces the $-HNm_1$ occurring in U by $-H_eNm_1$. U, S_{ep}, and $\mathcal{I}$ are ''state'' functions, in the sense that they depend on the state described by T, T_e, H, and, if needed, H_e. In the case where only one relevant effective parameter T_e remains, these functions do not depend on the path along which its value has been reached.

As we saw in [3] for the VFTH relaxing model at $T > T_0$ and in the Appendix for the Arrhenius relaxing case [see Eqs. (A25) and (A35)], the effective temperature alone is enough for a complete thermodynamic description of the dominant physical phenomena ($H_e = H$). The introduction of H_e becomes important only for second-order corrections in $\delta\mu_2$.

III. INHERENT STRUCTURE APPROACH

The characteristics of a glassy system may be represented by means of a multidimensional potential-energy function with a complex topography. The spatial patterns of atoms in crystals and in amorphous systems, at low temperature, represent minima in the potential-energy function describing the interactions [4,5].

In the case of the model (2.1), all the complex chemical properties of real glass formers do not occur, nevertheless, the system exhibits several aspects of their complex features, indicating that our simple model is complicated enough for what concerns the description and the comprehension of the basic long-time properties of a glass [3].

In a real glass, the presence of distinct processes (acting on different time scales) may be obtained from a careful analysis of the relaxation response function above T_g. We limit ourselves to a two-time-scale approach. This means that the deep and wide local minima at and below T_g are geometrically organized to create a two-scale-length potential-energy pattern. As a consequence, the system shows α and β processes. The α processes represent the escape from one deep minimum within a large scale valley to another valley. This escape requires a lengthy directed sequence of elementary transitions producing a very large activation energy. Moreover, the high-lying minima between any two valleys, among which the system is making a transition, are many and degenerate. This implies a large activation entropy for the *interbasin* transition. β processes are instead related to elementary relaxations between neighboring minima (*intrabasin* dynamics).

Note that in our models, we put together all kinds of β processes in our short time scale, since they are in any case much shorter than the observation time considered.

A. Decomposition of the partition function: Introduction of inherent structures

In this point of view, an approximate approach to the problem is to divide the complicated multidimensional landscape of the (potential) energy in structures formed by large deep basins and to describe the dynamics of the processes taking place as intrabasin and interbasin [4,5].

More precisely, one can define an inherent structure (IS) as that basin behind an actual configuration of the system evolving in time at some temperature T that is the minimum of the potential energy reached in an instantaneous quenching by the method of *steepest descent*.

The introduction of IS's allows, at low enough temperature ($T < T_g$), a decomposition of the partition function into an IS part, connected to the zero-temperature landscape corresponding to the configurations of the system at temperature T, and a part connected to the thermal excitation of the configurations in a single minimum.

The probability that an equilibrium configuration at $T = 1/\beta$ belongs to a basin associated with an IS structure with an energy density in the interval $[e, e+de]$ is [4,13,8,9]

$$\mathcal{P}(e,T)de \propto \exp\{-\beta N[e - Ts_c(e) + f_v(e,T)]\}de, \tag{3.1}$$

where $s_c(e)$ is proportional to the logarithm of the number of IS's existing at the energy level e and $f_v(e,T)$ is the free energy of the configurations inside an IS at energy e (related to a temperature T system). To derive the distribution (3.1) in this form the approximation is made that f_v is computed as the average over all the IS's of energy e. This means that, by assumption, the shape of a basin depends only on its energy level and on the temperature. Enough below T_g the further approximation may be made, that $f_v(e,T) \sim f_v(T)$, because fluctuations inside one IS are small [12,13]. The shape of the basin depends, then, only on the temperature. All the internal (vibrational) states of any IS have the same (vibrational)

free-energy f_v at given T. We anticipate, however, that in the present study, we will not carry out such an approximation for our models.

IS dynamics are significant, i.e., they significantly represent the actual dynamics of the system at finite T, provided that there is a one-to-one correspondence between IS's and real minima of the thermodynamic potential at finite temperature and provided that these IS's are visited with the same frequency with which the corresponding finite T minima are visited.

B. How it is carried out in mean-field spherical *p*-spin model

For what concerns disordered spin systems, in order to find the stable solutions, the TAP [14] approach may be used. Following this approach, for fixed quenched disorder, the spin fluctuations are averaged out, leaving self-consistent equations for the averages of the spins, i.e., the local magnetizations. These equations may be derived by a variation of a mean-field free-energy functional of the local magnetizations. The solutions of TAP equations (TAP states or pure states) are, therefore, minima of the free-energy landscape, once that the fluctuations have been eliminated performing an average. Every TAP state is characterized by a set of local magnetizations m_i, where $i=1,\ldots,N$ and N is the size of the system. The inherent structures, then, follows from TAP construction in the limit of the temperature going to zero.

C. Inherent structure approach in the harmonic-oscillator spherical spin model

As we will see, the model (2.1) is built in such a way that every $\{x_i\}$ configuration is an inherent structure. Indeed, at a given $\{x_i\}$ configuration at finite T, the $\{S_i\}$ are fast variables and they contribute to the energy and to the other observables as a noise depending on temperature. If we take away this contribution, we do not actually change the configurations of the minima of the slow variables. In the case of the system without constraint on the configuration space, nor contrived dynamics (see Sec. II C 2), any $\{x_i\}$ configuration is an inherent structure. For what concerns the constrained model, instead, certain configurations are not allowed (Sec. II C 1). Moreover, the presence of the constraint (2.9) produces (entropic) barriers higher than in the other case to get from a certain IS to a different one. That just means that the dynamics through the inherent structures is even slower in the fragile glass case than in the strong glass case.

First of all, we have to define the steepest descent procedure for the model. We start performing the minimization of

$$\mathcal{H}+\lambda\sum_{i=1}^{N} S_i^2-\lambda N, \tag{3.2}$$

where $\mathcal{H}$ is the Hamiltonian (2.1) of the model and where we implemented the spherical constraint $\Sigma_i S_i^2=N$ by using the Lagrange multiplier λ.

To get rid of the contribution of the spins, i.e., to get rid of the fast modes, we minimize Eq. (3.2) with respect to the $\{S_i\}$. We get

$$S_i^{(\min)}=\frac{Jx_i+L}{2\lambda} \quad \forall i. \tag{3.3}$$

Inserting this value for S_i and solving the spherical condition $\Sigma_{i=1}^{N}(S_i^{\min})^2=N$ for λ, we find

$$\lambda=\frac{w_{\rm is}}{2}, \tag{3.4}$$

where m_1 and m_2 are defined in Eq. (2.3) and

$$w_{\rm is}\equiv\sqrt{J^2m_2+2JLm_1+L^2}. \tag{3.5}$$

Using Eqs. (3.4), the minimum $\{S_i\}$ configuration for a given set of $\{x_i\}$ is, thus, given by

$$S_i^{(\min)}=\frac{Jx_i+L}{w_{\rm is}} \quad \forall i. \tag{3.6}$$

Finally, the expression (3.2) becomes

$$\mathcal{H}_{\rm is}\equiv N\left[\frac{K}{2}m_2-Hm_1-w_{\rm is}\right] \tag{3.7}$$

that is the energy function of the inherent structures. Consequently, the partition sum over inherent structures is defined by

$$Z_{\rm is}=\int \mathcal{D}x\,\exp[-\beta\mathcal{H}_{\rm is}]=\int dm_1\,dm_2\,\exp(\mathcal{I}-\beta\mathcal{H}_{\rm is}). \tag{3.8}$$

Due to the minimization, any explicit dependence on T in the effective Hamiltonian disappears [compare Eqs. (2.5) and (3.7)]. In Eq. (2.2), we integrated over the spins, instead of minimizing with respect to them, and therefore we also had an entropic term $TS_{\rm ep}$ for the fast processes, with $S_{\rm ep}$ given in Eq. (2.8) and a slightly different internal energy [Nw instead of $Nw_{\rm is}$, with w given in Eq. (2.4) and $w_{\rm is}$ in Eq. (3.5)]. In the inherent structure approach, instead, carrying out the steepest descent makes the entropic term vanish (only the minimal configuration is taken into account) and the effective Hamiltonian, given in Eq. (3.7), has no explicit dependence on the temperature. All by all, we notice a close analogy with the inherent structures in the spherical p-spin model: in both cases, one may sum out fast processes at finite T, and then send the temperature to zero to get the inherent structures.

The configurational entropy for IS's comes from the Jacobian of the transformation of variables $\mathcal{D}x=e^{\mathcal{I}}dm_1\,dm_2$ [see Eqs. (2.3) and (2.14)]. It is the same of the finite T case, since any allowed configuration $\{x_i\}$ is also an IS.

The static average of $\mathcal{H}_{is}$ is given by

$$E_{\rm eq}^{\rm is}(T)=\mathcal{H}_{is}[\overline{m}_{1,2}^{(\rm is)}(T)], \tag{3.9}$$

where $\overline{m}_{1,2}^{(\rm is)}(T)$ are the solutions of the saddle-point equations that we get in the IS case to compute Eq. (3.8), in the limit of large N. The equations are

$$\overline{m}_1^{(\mathrm{is})} = \frac{D}{J(K - J^2/w_{\mathrm{is}})} - \frac{L}{J} = \frac{\tilde{H}_{\mathrm{is}}}{\tilde{K}_{\mathrm{is}}}, \tag{3.10}$$

$$\overline{m}_2^{(\mathrm{is})} - (\overline{m}_1^{(\mathrm{is})})^2 = \frac{T}{D}(J\overline{m}_1^{(\mathrm{is})} + L) = \frac{T}{\tilde{K}_{is}}, \tag{3.11}$$

where we define

$$\tilde{H}_{\mathrm{is}} \equiv H + \frac{JL}{w_{\mathrm{is}}}; \quad \tilde{K}_{\mathrm{is}} \equiv K - \frac{J^2}{w_{\mathrm{is}}}, \tag{3.12}$$

with w_{is} from Eq. (3.5). The combination $\tilde{H}_{\mathrm{is}}J + \tilde{K}_{\mathrm{is}}L = HJ + KL = D$ is, again, simple, as in Eq. (2.12).

In the case at finite T, the static partition function (2.13) was

$$Z = \int dm_1\, dm_2 \exp(\mathcal{I} - \beta \mathcal{H}_{\mathrm{eff}}), \tag{3.13}$$

with $\mathcal{H}_{\mathrm{eff}}$ defined in Eq. (2.5) and $\mathcal{I}$ in Eq. (2.14). The two saddle-point equations are different from Eqs. (2.15) and (2.16) valid in the realistic case, giving thus different results: $\overline{m}_{1,2}^{(\mathrm{is})} \neq \overline{m}_{1,2}$. We note explicitly that $\overline{m}_{1,2}^{(\mathrm{is})}$ depends on T even in the IS case.

Comparing the expressions so far obtained with those appearing in the exponent of the probability distribution (3.1) we identify the configurational entropy Ns_c with $\mathcal{I}$, as defined in Eq. (2.14), and the rest with

$$N(e + f_v) = \mathcal{H}_{\mathrm{eff}}(\{x_i\}) = \mathcal{H}_{\mathrm{is}}(\{x_i\}) + F_v(\{x_i\}), \tag{3.14}$$

where, as already told, $\mathcal{H}_{\mathrm{is}}(\{x_i\})$ is the IS internal energy and from the difference $\mathcal{H}_{\mathrm{eff}}(\{x_i\}) - \mathcal{H}_{\mathrm{is}}(\{x_i\}) = F_v(\{x_i\})$ the thermal free energy of one IS turns out to be

$$F_v = \frac{T}{2}\ln\left(\frac{w + T/2}{T}\right) - N(w - w_{is}), \tag{3.15}$$

where w is defined in (2.4) and w_{is} in (3.5). Notice that it explicitly depends on the parameters m_1 and m_2 of the IS, whereas in literature it is often assumed to be a constant (harmonic approximation [4,5,12,13,8,9]).

D. Effective temperature in the IS's approach

1. Expansion of the dynamical energy

A possible way of defining an effective temperature, sometimes used in literature, for instance in the study of Lennard-Jones interacting spheres [12,13] and in the study of the random orthogonal model [8], is to compare the time dependent out of equilibrium mean internal energy with the equilibrium mean internal energy expression at a temperature $T_e \neq T$. The out of equilibrium mean internal energy is built taking the dynamics of a system out of equilibrium at temperature T and repeating it many times starting from different initial conditions. A statistical ensemble of trajectories is constructed in this way. At any given time t, the configurations that each sample is visiting are found. The energy $\mathcal{H}_{\mathrm{is}}$ averaged over the ensemble of different trajectories is

$$E_d^{(\mathrm{is})}(t) \equiv \langle \mathcal{H}_{is} \rangle_t \equiv N\frac{K}{2} m_2(t) - NHm_1(t) - N\sqrt{J^2 m_2(t) + 2JLm_1(t) + L^2} \tag{3.16}$$

$$\simeq N\frac{K}{2}\overline{m}_2^{(\mathrm{is})} - NH\overline{m}_1^{(\mathrm{is})} - N\sqrt{J^2\overline{m}_2^{(\mathrm{is})} + 2JL\overline{m}_1^{(\mathrm{is})} + L^2} + N\tilde{K}_{is}(\overline{m}_1^{(\mathrm{is})}, \overline{m}_2^{(\mathrm{is})})\,\delta\mu_2(t) + C(\overline{m}_1^{(\mathrm{is})}, \overline{m}_2^{(\mathrm{is})})\,\delta\mu_2(t)^2, \tag{3.17}$$

where $\delta\mu_2(t) \equiv \mu_2(t) - \overline{\mu}_2(T)$ is given by Eq. (2.37) in the Arrhenius case and by Eq. (2.33) in the constrained case for $T \geqslant T_0$. The last three terms are

$$E_{\mathrm{eq}}^{(\mathrm{is})}(T) = N\frac{K}{2}\overline{m}_2^{(\mathrm{is})} - NH\overline{m}_1^{(\mathrm{is})} - N\sqrt{J^2\overline{m}_2^{(\mathrm{is})} + 2JL\overline{m}_1^{(\mathrm{is})} + L^2}. \tag{3.18}$$

The equilibrium IS energy $E_{\mathrm{eq}}^{(\mathrm{is})}(T)$ will be a different function of the temperature in the two dynamic versions of the model. The second-order expansion will be needed only for the strong glass case and the expression for the factor $C(\overline{m}_1^{(\mathrm{is})}, \overline{m}_2^{(\mathrm{is})})$ is, in that case

$$C(\overline{m}_1^{(\mathrm{is})}, \overline{m}_2^{(\mathrm{is})}) = \frac{DJ^4K^2}{8(D + J^2)^4}. \tag{3.19}$$

We may then take a system in equilibrium at a temperature T_e, such that the configurations visited by the system at equilibrium are the same as those out of equilibrium at temperature T. This we call effective temperature. To be more precise, fixing t, T_e is defined as the temperature at which the system at equilibrium would visit the same configurations visited by the system out of equilibrium at temperature T, with the same frequency.

2. The effective temperature employed in numerical approaches: The fragile case

Following the approach found in literature [12,13,8] for numerical simulations, we may define a $T_{e1}^{(\mathrm{is})}$ through the matching of the equilibrium and the out-of-equilibrium IS internal energy: it is the one such that

$$E_{\mathrm{eq}}^{(\mathrm{is})}[T_{e1}^{(\mathrm{is})}(t)] = E_d^{(\mathrm{is})}(t). \tag{3.20}$$

For our paper, it is possible to work out an analytic expression for such a $T_{e1}^{(\mathrm{is})}(t)$, at least near the Kauzmann transition for the fragile glass case, linearizing in $T - T_0$.

What we get is a parameter different from the thermodynamic effective temperature (2.41) that we got from three different approaches (including the Fluctuation-Dissipation Ratio) in [3].

For the fragile glass case, we are not able to derive any simple expression, of the IS energy (3.16), but we may in

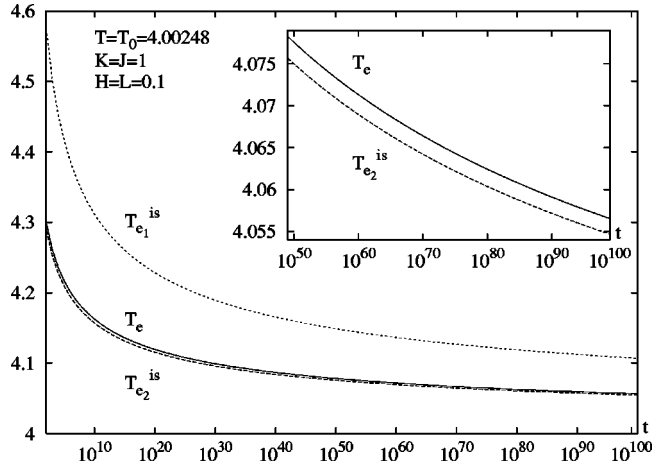

FIG. 1. Effective temperatures vs t at the heat bath temperature $T=4.002\,48$, equal to the Kauzmann temperature. The constants in the Hamiltonian (2.1) are set to the following values: $K=J=1$, $H=L=0.1$. The constraint constant is $m_0=5$. The upper curve shows the effective temperature got by matching out of equilibrium and equilibrium IS internal energy. The one in the middle is the behavior of Eq. (2.41), for systems at finite T, and the lowest one is the IS effective temperature (3.29).

any case solve it exactly. The results are shown in Figs. 1 and 2 for a given choice of the values of the interaction parameters and of the VFTH exponent of the model. As one can see, $T_{e1}^{(\mathrm{is})}(t)$ turns out to be different from $T_e(t)$ at any time decade.

As a matter of fact, what we are comparing now with the average $E_d(t)$ is a function $E_{\mathrm{eq}}(T_{e1}^{(\mathrm{is})})$ of the effective temperature alone, while we know that out of equilibrium, any proper thermodynamic function cannot simply depend on just one temperature as the thermodynamic functions of equilibrium systems do [25]. It is not surprising, thus, that the two functions do not coincide.

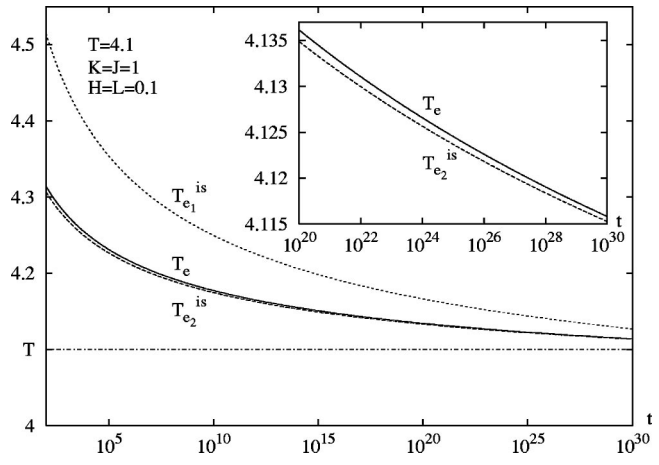

FIG. 2. The same effective temperatures, for the same choice of parameters as before are plotted for a different heat bath temperature: $T=4.1$.

3. The effective temperature employed in numerical approaches: The strong case

For the strong glass case, it is possible to work out a simple analytic expression for the dynamical and the equilibrium IS energy. To do it, we will expand near zero temperature up to second order in T.

We underline that the thermodynamic effective temperature given in Eq. (2.41) is also the expression of the effective temperature for the system without constraint. What changes in that case is the time behavior of $m_2-m_1^2=\mu_2$, that is now given by Eq. (2.36), and its limit at equilibrium [see Eq. (2.16)]. In this case, where the analytic treatment is, by far, easier, we can give a short explicit expression for $T_{e1}^{(\mathrm{is})}(t)$:

$$T_{e1}^{(\mathrm{is})} \simeq T + \frac{KD}{D+J^2}\,\delta\mu_2(t) + \frac{J^4K^2}{2(D+J^2)^3}\,T\,\delta\mu_2(t) + O(T^3) + O(\delta\mu_2(t)^3). \tag{3.21}$$

Here, terms of $O(T^2)$ and $O(\delta\mu_2(t)^2)$ cancel. This $T_{e1}^{(\mathrm{is})}(t,T)$ is obtained from Eq. (3.20) with

$$\frac{E_{\mathrm{d}}^{\mathrm{is}}(t)}{N} \simeq -\frac{(H+J)^2}{2K} - L + \frac{T}{2} - \frac{J^4K}{8D(D+J^2)^2}\,T^2 + \frac{KD}{2(D+J^2)}\,\delta\mu_2(t) + \frac{J^4K^2}{8D(D+J^2)^2}\,T\,\delta\mu_2(t) + \frac{DJ^4K^3}{8(D+J^2)^4}\,\delta\mu_2(t)^2 + O(T^3) + O(T^2\delta\mu_2(t)) + O(T\delta\mu_2(t)^2) + O(\delta\mu_2(t)^3). \tag{3.22}$$

If we expand (2.41) in the same way, we get

$$T_e = T + \tilde{K}\,\delta\mu_2(t) = T + \frac{KD}{D+J^2}\,\delta\mu_2(t) + \frac{T}{2}\left(\frac{JK}{D+J^2}\right)^2\delta\mu_2(t) + \frac{DJ^4K^3}{2(D+J^2)^4}\,\delta\mu_2(t)^2 + O(T^3) + O[T^2\delta\mu_2(t)] + O[T\delta\mu_2(t)^2] + O[\delta\mu_2(t)^3]. \tag{3.23}$$

As we see from the formulas above, and from Figs. 3 and 4, for a given choice of the parameter values, in the case with Arrhenius relaxation T_e and $T_{e1}^{(\mathrm{is})}$ are very similar. Their difference is one order of magnitude less than in the model with contrived dynamics.

4. A more fundamental definition of the IS effective temperature

Here, we propose an alternative way to identify an effective temperature that maps the dynamics between inherent structures into a thermodynamic quantity. We follow a quasistatic approach using a partition sum, just as we did in the finite T case. The aim is to be able to define an effective thermodynamic parameter for the IS dynamics and to compare it with the T_e given in Eq. (2.41). Following exactly the

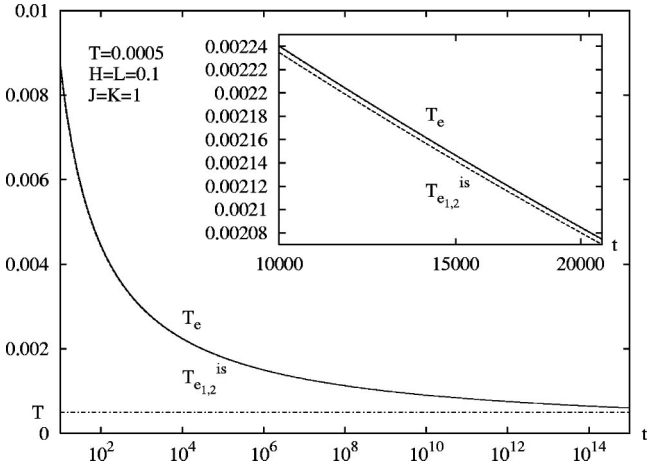

FIG. 3. Time evolution of the effective temperatures at the heat bath temperature $T=0.0005$ in the model with Arrhenius relaxation. The constants in the Hamiltonian (2.1) are set to the following values: $K=J=1$, $H=L=0.1$. The lower curve shows the effective temperature (3.21) got by matching out of equilibrium and equilibrium IS internal energy. To order $\delta\mu_2$ it coincides analytically with the IS effective temperature (3.34). Second-order differences are too small to appear in the plot. The upper curve is the behavior of Eq. (2.41), for systems at finite T.

same approach we used in [3] (see Sec. II D), including the substitution of the real external field H with the effective one $H_{e2}^{(\mathrm{is})}$, we compute the partition function counting all the macroscopically equivalent IS's, through which the system is evolving in this symbolic dynamics, at a given time t.

$$Z_e^{(\mathrm{is})}(m_1,m_2)=\int \mathcal{D}x\,\exp[-\beta_{e2}^{(\mathrm{is})}\mathcal{H}_{\mathrm{is}}(\{x_i\};T,H_{e2}^{(\mathrm{is})})]\times\delta\left(Nm_1-\sum_i x_i\right)\delta\left(Nm_2-\sum_i x_i^2\right) \quad (3.24)$$

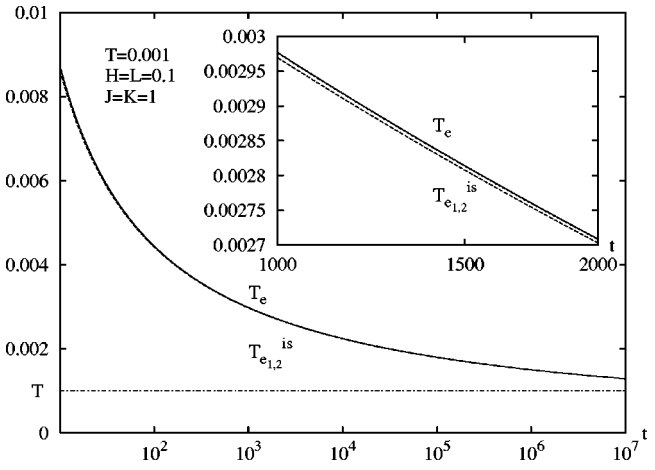

FIG. 4. The same effective temperatures, for the same choice of parameters as before are plotted for a different heat bath temperature: $T=0.001$. Comparing the time scales of the two plots, we can clearly observe the decreasing of the Arrhenius relaxation time to equilibrium τ_{eq} that takes places raising the temperature.

$$=\exp\left\{-\beta_{e2}^{(\mathrm{is})}N\left[\frac{K}{2}m_2-H_{e2}^{(\mathrm{is})}m_1-\overline{w}_{\mathrm{is}}-\frac{T_{e2}^{(\mathrm{is})}}{2}\ln(m_2-m_1^2)\right]\right\} \quad (3.25)$$

$$\simeq\exp\{-\beta_{e2}^{(\mathrm{is})}[\mathcal{H}_{\mathrm{is}}(m_1,m_2;T,H_{e2}^{(\mathrm{is})})-T_{e2}^{(\mathrm{is})}\mathcal{I}(m_1,m_2)]\}. \quad (3.26)$$

$\beta_{e2}^{(\mathrm{is})}=1/T_{e2}^{(\mathrm{is})}$ and $H_{e2}^{(\mathrm{is})}$ are parameters describing the behavior of the system going only through IS's. Minimizing the free energy $F_e^{(\mathrm{is})}\equiv -T_{e2}^{(\mathrm{is})}\ln Z_e^{(\mathrm{is})}$ with respect to $m_{1,2}$ we get

$$T_{e2}^{(\mathrm{is})}=\tilde{K}_{\mathrm{is}}(m_1,m_2)[m_2-m_1^2], \quad (3.27)$$

$$H_{e2}^{(\mathrm{is})}=H-\tilde{K}_{\mathrm{is}}(m_1,m_2)\mu_1. \quad (3.28)$$

By inserting the time-dependent values of m_1 and m_2 we now look at the time evolution of the effective temperature (3.27) for large times, in the aging regime, and we compare it with the behavior of the thermodynamic effective temperature (2.41).

For the dynamically constrained model, for $t\to\infty$, $T_{e2}^{(\mathrm{is})}\to T$ (if $T>T_0$). When $t_0\ll t<\infty$, however, the way the effective temperature approaches the heat-bath temperature is different from the behavior (2.41) of T_e, found in the case at finite temperature. For a comparison, their first-order expansions are

$$T_{e2}^{(\mathrm{is})}\simeq T+\left(1+T\frac{\tilde{K}_{\mathrm{is},\infty}(T)Q_\infty^{(\mathrm{is})}J^2}{2D(1+Q_\infty^{(is)}D)}\right)\tilde{K}_{\mathrm{is},\infty}(T)\,\delta\mu_2(t), \quad (3.29)$$

$$T_e\simeq T+\left(1+T\frac{\tilde{K}_\infty(T)Q_\infty J^2}{2D(1+Q_\infty D)}\right)\tilde{K}_\infty(T)\,\delta\mu_2(t), \quad (3.30)$$

with

$$\tilde{K}_{\mathrm{is},\infty}(T)=\lim_{t\to\infty}\tilde{K}_{\mathrm{is}}[m_1(t),m_2(t);T], \quad (3.31)$$

$$\tilde{K}_\infty(T)=\lim_{t\to\infty}\tilde{K}[m_1(t),m_2(t);T],$$

$$Q_\infty^{(\mathrm{is})}=\lim_{t\to\infty}\frac{J^2D}{\tilde{K}_{\mathrm{is}}^3w_{\mathrm{is}}^3}, \quad (3.32)$$

$$Q_\infty=\lim_{t\to\infty}Q=\lim_{t\to\infty}\frac{J^2D}{\tilde{K}^3w(w+T/2)^2}. \quad (3.33)$$

The time-dependent variable $\delta\mu_2(t)$ [introduced in Eq. (2.33)] is the same in both cases (apart from the parameter t_0 influencing only the short times) while the coefficients in front of it are different at any temperature, including T_0. In the fragile case, thus, this second IS effective temperature does not coincide with $T_{e1}^{(\mathrm{is})}$ and it is much nearer, at any

time, to Eq. (3.30). However, even if this $T_{e2}^{(\mathrm{is})}$ is conceptually more properly chosen than the one defined matching out of equilibrium energy at temperature T and equilibrium energy at temperature $T_{e1}^{(is)}$, we still do not get the same parameter describing the finite T dynamics in a thermodynamic frame. The inherent structure approach gives thus a good approximation but is nevertheless never analytically correct in the description of the real temperature dynamics. To show how good this approximation is, we may take as an instance a certain realization of the model with given values of the ''fields'' and ''coupling constants.'' We plot in Figs. 1 and 2 the behavior of $T_{e1}^{(\mathrm{is})}(t)$, $T_{e2}^{(\mathrm{is})}(t)$, and $T_e(t)$ at heat-bath temperatures equal to and just above the Kauzmann temperature.

For the strong glass case, we also expand for temperatures near to zero and for long time and we get

$$T_{e2}^{(\mathrm{is})}(t)=T+\tilde{K}_{\mathrm{is}}\delta\mu_2(t)=T+\frac{KD}{D+J^2}\delta\mu_2(t)+\frac{T}{2}\frac{J^4K^2}{(D+J^2)^3}\delta\mu_2(t)+\frac{DJ^4K^3}{2(D+J^2)^4}\delta\mu_2(t)^2+O(T^3)+O[T^2\delta\mu_2(t)]+O[T\delta\mu_2(t)^2]+O[\delta\mu_2(t)^3] \tag{3.34}$$

$$=T_e(t)-\frac{DJ^2K^2}{2(D+J^2)^3}T\delta\mu_2(t)+O[\delta\mu_2(t)^3]+O(T^3)+O[T^2\delta\mu_2(t)]+O[T\delta\mu_2(t)^2] \tag{3.35}$$

$$=T_{e1}^{(\mathrm{is})}(t)+\frac{DJ^4K^3}{2(D+J^2)^4}\delta\mu_2(t)^2+O(T^3)+O[T^2\delta\mu_2(t)]+O[T\delta\mu_2(t)^2]+O[\delta\mu_2(t)^3], \tag{3.36}$$

where $\delta\mu_2(t)$ is given by Eq. (2.37).

The effective temperature T_e mapping the dynamics of the system evolving at finite-temperature T have the same behavior of T_{e2} in approaching the heat-bath temperature up to order $T\delta\mu_2(t)$ where they start deviating one from the other. For a quenching to zero temperature, the two effective temperatures coincide. Moreover, due to the simplicity of the model, the IS effective temperature $T_{e2}^{(\mathrm{is})}$ is equal to $T_{e1}^{(\mathrm{is})}$ given in Eq. (3.21) up to order $\delta\mu_2(t)$ in time and up to order T^2 in temperature.

IV. CONCLUSIONS

In this paper, we consider a model that owns all the basic properties of a glass, built by processes evolving on two well-separated time scales, representing the α and β processes taking place in real glassy materials [3]. The decoupling of time scales is fundamental for a generalization of equilibrium thermodynamics to systems far from equilibrium.

We take into account two different versions of the model given by Eq. (2.1). One leading to the description of a fragile glass having a nonzero Kauzmann temperature and the other one representing a strong glass.

Using a particular Monte Carlo dynamics and developing it analytically, thus having the opportunity of probing it in more detail with respect to a numerical study, we found equations of motion that are in all respect those typical of glass relaxation.

In the strong glass case, we apply exactly the same parallel Monte Carlo dynamics used in [16–18,25], finding an Arrhenius relation between the relaxation time of the slow processes $\{x_i\}$ and the temperature.

In the fragile glass case, the model is provided with a constraint applied to the harmonic-oscillator dynamics, i.e., to the slow processes dynamics, in order to reproduce the behavior of a good fragile glass former. In [3], by means of a Monte Carlo constrained dynamics, we identified the Kauzmann temperature with the one T_0 at which the constraint is reached, for the first time in a cooling experiment from high temperature. There we showed how the thermodynamic phase transition [27], that takes place due to the breaking of the ergodicity in the landscape of our model, is characterized.

In this paper, we carried out the inherent structure approach. In both dynamical models, decreasing the temperature, the free-energy local minima do not split into smaller local minima, just like in the *p*-spin model in zero magnetic field [11], because every allowed configuration of harmonic oscillators is and remains an inherent structure at any temperature. Consequently, we may set a one-to-one correspondence between the minima of the free energy and the ones of the potential energy (i.e., the inherent structures). Because of this exact correspondence, the dynamics through inherent structures should be a valid symbolic dynamics for the real system, i.e., at a finite heat-bath temperature T. At least, it would significantly represent the actual dynamics if the inherent structures are visited with the same frequency with which the corresponding free-energy minima at finite T are visited.

In our paper, the proper way to define IS's is to minimize the model Hamiltonian [Eq. (2.1)] with respect to the spherical spins, i.e., the fast relaxing variables. Performing such a minimization, we get the effective Hamiltonian given by Eq. (3.7) instead of the one given by Eq. (2.5), where Eq. (3.7) is just Eq. (2.5) for $T=0$: due to the minimization any explicit dependence on T disappears. The configurational entropy for inherent structures was computed from the logarithm of the Jacobian of the transformation of variables $\mathcal{D}x\rightarrow dm_1\,dm_2$, and thus it was the same of the exact finite T approach. In our models, then, any configuration of harmonic-oscillators $\{x_i\}$ (for the fragile glass model, every configuration allowed by the constraint), is also an inherent structure. Although the models we considered are conceptually very simple and without interactions, as compared to another approach proposed for systems with interacting discrete spins where the IS scheme breaks down [28], our setup seems to be more physical since it is intimately based on time scale separation between fast and slow processes. A direct consequence of this time scale separation is that we encounter both a math-

ematically and physically well-defined configurational entropy, whereas this observable suffers from principle difficulties in other approaches [28].

We may take a system in equilibrium at an effective temperature $T_e^{(\mathrm{is})}$, such that the configurations visited by the system at equilibrium are the same as those out of equilibrium at temperature T. First, we defined an effective temperature through the matching of the equilibrium and the out-of-equilibrium internal energy of the inherent structures [the one such that $E(T_e^{(\mathrm{is})}(t))=E_d(t)$]. For the strong glass model, this effective temperature almost coincides with T_e provided that the temperature at which the system is quenched is not too high [as far as terms of $O(T\delta\mu_2(t))$ are negligible they are equal]. On the contrary, when the constraint is set and the contrived Monte Carlo dynamics is applied, we found that the thus derived effective temperature $T_{e1}^{(\mathrm{is})}$ is quite different from the effective temperature that we were able to identify in the finite T dynamics. Therefore, we proposed a definition following a quasistatic approach. In this way, we computed the partition function counting all the macroscopically equivalent inherent structures, through which the system is evolving in this symbolic dynamics, at a given time t. Even though the result we get is much more similar to the finite T dynamics effective temperature (numerically speaking the difference is one order of magnitude smaller), yet it is analytically different, indicating that the inherent structure scheme for the study of dynamics can only be an approximation to what happens in the realistic dynamics of the system. As a consequence, also the derivation of out-of-equilibrium thermodynamic quantities (e.g., the configurational entropy) obtained making use of this approach could suffer of a systematic deviation from the exact result.

ACKNOWLEDGMENTS

We thank F. Ritort for suggestions and a careful reading of the manuscript. We also thank A. Crisanti and F. Sciortino for useful discussions. The research of L. Leuzzi is supported by FOM (The Netherlands).

APPENDIX: STRONG GLASS DYNAMICS

In this Appendix, we present the Monte Carlo dynamics of the observables μ_1 and μ_2, functions of the slow relaxing harmonic-oscillators $\{x_i\}$ through

$$m_1=\frac{1}{N}\sum_i x_i, \quad m_2=\frac{1}{N}\sum_i x_i^2, \tag{A1}$$

in the case where the model (2.1) is not subjected to any constraint on its $\{x_i\}$ configurations.

Let us recall the definitions, given in Sec. II C,

$$\mu_1\equiv\frac{\tilde{H}}{\tilde{K}}-m_1, \tag{A2}$$

$$\mu_2\equiv m_2-m_1^2. \tag{A3}$$

In this notation, the average and the variance (2.23) of the Gaussian distribution $p(x|m_1,m_2)$ [see (2.21)] of the possible changes in energy during the Monte Carlo dynamics become

$$\overline{x}=\frac{\Delta^2\tilde{K}}{2}, \quad \Delta_x=\Delta^2\tilde{K}^2(\mu_2+\mu_1^2). \tag{A4}$$

We remember that x is the difference (2.20) between the energy of the configuration proposed for the exchange and the energy of the actual configuration. Δ is fixed.

To shorten the following expressions, we also define the parameter:

$$\alpha\equiv\frac{\overline{x}}{\sqrt{2\Delta_x}}=\sqrt{\frac{\Delta^2}{8(\mu_2+\mu_1^2)}}. \tag{A5}$$

The two basic quantities that have to be computed in order to solve the dynamic equations for μ_1 and μ_2 are the acceptance rate of the Monte Carlo updating

$$A(t)\equiv\int dx\, W(\beta x)p(x|m_1,m_2), \tag{A6}$$

and the rate of change of the energy of the system,

$$I_1(t)\equiv\int dx\, xW(\beta x)p(x|m_1,m_2). \tag{A7}$$

Defining the auxiliary function

$$f(t)\equiv\overline{x}\beta\exp\left(-\beta\overline{x}+\frac{\beta^2\Delta_x}{2}\right)\mathrm{erfc}\left(\sqrt{\frac{\Delta_x}{\overline{x}}}\beta-\alpha\right), \tag{A8}$$

where

$$\mathrm{erfc}(a)\equiv\frac{2}{\sqrt{\pi}}\int_a^\infty dz\, e^{-z^2}, \tag{A9}$$

we can write down the exact expressions for A and I_1 as

$$A=\frac{1}{2}\left[\mathrm{erfc}(\alpha)+\frac{f}{\beta\overline{x}}\right], \tag{A10}$$

$$I_1=\frac{\overline{x}}{2}\left[\mathrm{erfc}(\alpha)+\left(1-\frac{\beta\overline{x}}{2\alpha^2}\right)\frac{f}{\beta\overline{x}}\right]. \tag{A11}$$

The Monte Carlo equations of motion for μ_1 and μ_2 are formally the same found for the fragile glass case [3]

$$\dot{\mu}_1=-JQ\int dx\, xW(\beta x)p(x|m_1,m_2) -(1+DQ)\int dx\,\overline{y}(x)W(\beta x)p(x|m_1,m_2), \tag{A12}$$

$$\dot{\mu}_2 = \frac{2}{\tilde{K}} \int dx x W(\beta x) p(x|m_1, m_2) + 2\mu_1 \int dx \, \overline{y}(x) W(\beta x) p(x|m_1, m_2). \quad \text{(A13)}$$

From Eq. (2.23), we know $\overline{y}(x)$ and we may rewrite it as a function of the above-defined α and $\overline{x}$:

$$\overline{y}(x) = 4\alpha^2 \mu_1 \left(1 - \frac{x}{\overline{x}} \right). \quad \text{(A14)}$$

Using this, we get

$$\dot{\mu}_1 = -\left(JQ - \frac{8\alpha^2 \mu_1 (1+DQ)}{\Delta^2 \tilde{K}} \right) I_1(t) - 4\alpha^2 \mu_1 (1+DQ) A(t), \quad \text{(A15)}$$

$$\dot{\mu}_2 = \frac{2}{\tilde{K}} \left(1 - \frac{8\alpha^2 \mu_1^2}{\Delta^2 \tilde{K}} \right) I_1(t) + 8\alpha^2 \mu_1^2 A(t). \quad \text{(A16)}$$

1. Dynamics in the aging regime: Zero temperature

First of all, we solve the equation of motion for μ_2 at $T=0$, neglecting terms of order μ_1^2 with respect to those of order μ_2. For long times $\alpha \gg 1$. We can, then, expand $I_1(t)$ for large α, getting

$$I_1(t) \simeq -\frac{e^{-\alpha^2}}{2\alpha\sqrt{\pi}} \frac{\Delta^2 \tilde{K}}{4\alpha^2}. \quad \text{(A17)}$$

Equation (A16) becomes then

$$\dot{\mu}_2 \simeq -\frac{e^{-\alpha^2}}{2\alpha\sqrt{\pi}} \frac{\Delta^2}{4\alpha^2}, \quad \text{(A18)}$$

otherwise written as

$$\dot{\alpha} \simeq \frac{e^{-\alpha^2}}{\sqrt{\pi}}, \quad \text{(A19)}$$

or

$$\dot{\mu}_2 \simeq -2\mu_2^{3/2} \frac{\exp\left(-\frac{\Delta^2}{8\mu_2} \right)}{\sqrt{\pi}}. \quad \text{(A20)}$$

At $T=0$, the solution in the aging regime, expressed in $\mu_2 \simeq \Delta^2/(8\alpha^2)$, turns out to be

$$\mu_2(t) \simeq \frac{\Delta^2}{8} \frac{1}{\ln \frac{2t}{\sqrt{\pi}} + \frac{1}{2} \ln \ln \frac{2t}{\sqrt{\pi}}}. \quad \text{(A21)}$$

Always at zero temperature, the leading order of the expansion of the acceptance rate A is, for $\alpha \gg 1$,

$$A \simeq \frac{e^{-\alpha^2}}{2\alpha\sqrt{\pi}}. \quad \text{(A22)}$$

Combining this with Eq. (A17), the Monte Carlo equation of motion (A15) takes the form

$$\dot{\mu}_1 = \frac{e^{-\alpha^2}}{2\alpha\sqrt{\pi}} \left\{ \frac{JQ\Delta^2 \tilde{K}}{4\alpha^2} - 2\mu_1 (1+DQ)(2\alpha^2+1) \right\}. \quad \text{(A23)}$$

Dividing Eq. (A23) by Eq. (A18), we may write down a differential equation for μ_1 as a function of μ_2

$$\frac{d\mu_1}{d\mu 2} \simeq 16(1+DQ) \frac{\alpha^4}{\Delta^2} \mu_1 - JQ\tilde{K}, \quad \text{(A24)}$$

where we have neglected terms of order $1/\alpha^2$ with respect to those of order one. In the adiabatic approximation, obtained by neglecting the left-hand side, the solution of Eq. (A24) turns out to be

$$\mu_1 \simeq \frac{4JQ\tilde{K}}{\Delta^2 (1+DQ)} \mu_2^2. \quad \text{(A25)}$$

At zero temperature and for long times, one thus has $\mu_1 \sim \mu_2^2 \ll \mu_2$.

2. Dynamics in the aging regime: $T>0$

If T is above zero, the leading order of the expansion of A and I_1 for large times ($\alpha \gg 1$) and small temperature are

$$A \simeq \frac{e^{-\alpha^2}}{2\alpha\sqrt{\pi}} \frac{1}{1 - \frac{4T\alpha^2}{\Delta^2 \tilde{K}}}, \quad \text{(A26)}$$

$$I_1 \simeq \frac{e^{-\alpha^2}}{2\alpha\sqrt{\pi}} \frac{\Delta^2 \tilde{K}}{4\alpha^2} \frac{1 - \frac{8T\alpha^2}{\Delta^2 \tilde{K}}}{\left(1 - \frac{4T\alpha^2}{\Delta^2 \tilde{K}} \right)}, \quad \text{(A27)}$$

where the terms $T\alpha^2$ are of $O(1)$. Indeed, it is

$$\frac{8T\alpha^2}{\Delta^2 \tilde{K}} = \frac{8T}{\Delta^2 \tilde{K}} \frac{\Delta^2}{8\mu_2} = \frac{\overline{\mu}_2}{\mu_2} = \frac{1}{1 + \frac{\delta\mu_2}{\overline{\mu}_2}}, \quad \text{(A28)}$$

[see the definition of α (A5)], so that

$$\lim_{t \to \infty} \frac{8T\alpha^2}{\Delta^2 \tilde{K}} = 1, \quad T>0. \quad \text{(A29)}$$

In this notation, Eqs. (A26) and (A27) may be rewritten also as

$$A=\frac{e^{-\alpha^2}}{\alpha\sqrt{\pi}}\frac{1+\frac{\delta\mu_2}{\overline{\mu}_2}}{1+2\frac{\delta\mu_2}{\overline{\mu}_2}}, \tag{A30}$$

$$I_1=-\frac{e^{-\alpha^2}}{\alpha\sqrt{\pi}}\frac{\Delta^2\tilde{K}}{\alpha^2}\frac{\delta\mu_2}{\overline{\mu}_2}\frac{1+\frac{\delta\mu_2}{\overline{\mu}_2}}{\left(1+2\frac{\delta\mu_2}{\overline{\mu}_2}\right)^2} \tag{A31}$$

and the Monte Carlo equations are now

$$\dot{\mu}_1\simeq\frac{e^{-\alpha^2}}{\alpha\sqrt{\pi}}\frac{1+\frac{\delta\mu_2}{\overline{\mu}_2}}{1+2\frac{\delta\mu_2}{\overline{\mu}_2}}\left[-4\alpha^2(1+DQ)\mu_1+\frac{JQ\Delta^2\tilde{K}}{2\alpha^2}\frac{\delta\mu_2}{\overline{\mu}_2}\frac{1}{1+2\frac{\delta\mu_2}{\overline{\mu}_2}}\right], \tag{A32}$$

$$\dot{\mu}_2\simeq\frac{e^{-\alpha^2}}{\alpha\sqrt{\pi}}\frac{\Delta^2}{\alpha^2}\frac{\delta\mu_2}{\overline{\mu}_2}\frac{1+\frac{\delta\mu_2}{\overline{\mu}_2}}{\left(1+2\frac{\delta\mu_2}{\overline{\mu}_2}\right)^2}. \tag{A33}$$

The solution to Eq. (A33) is, to leading order,

$$\mu_2(t)\simeq\frac{\Delta^2}{8}\frac{1}{\ln\frac{2t}{\sqrt{\pi}}}. \tag{A34}$$

The behavior of μ_1 comes out to be

$$\mu_1\simeq\frac{4JQ\tilde{K}}{\Delta^2(1+DQ)}\mu_2^2\frac{\delta\mu_2}{\overline{\mu}_2}\frac{2}{1+2\frac{\delta\mu_2}{\overline{\mu}_2}}. \tag{A35}$$

Notice that this vanishes when equilibrium is approached, since then $\delta\mu_2\to 0$.

For times even longer than the time scale of the aging regime, the system finally relaxes, exponentially fast, to equilibrium. The equilibrium value of μ_2 is known from the statics (see Sec. II), as

$$\overline{\mu}_2=\frac{T}{\tilde{K}_\infty(T)}, \tag{A36}$$

where the explicit expansion of $\tilde{K}_\infty(T)$ in temperature is shown in Eq. (2.38). The asymptotic value of α is, from its definition (A5) and taking the first-order expansion in T,

$$\alpha(T)=\sqrt{\frac{\Delta^2}{8\overline{\mu}_2(T)}}\simeq\sqrt{\frac{A_s}{T}}, \tag{A37}$$

with

$$A_s\equiv\frac{\Delta^2 KD}{8(D+J^2)}. \tag{A38}$$

From the equations of motion studied above [look for instance at Eq. (A19)], we find for the relaxation time to equilibrium

$$\tau_{eq}\propto e^{\alpha^2}. \tag{A39}$$

Using Eq. (A37), this is nothing else than the Arrhenius law

$$\tau_{eq}\sim\exp\left(\frac{A_s}{T}\right). \tag{A40}$$

[1] C. A. Angell, Science **267**, 1924 (1995).
[2] G. B. McKenna, in *Comprehensive Polymer Science 2: Polymer Properties*, edited by C. Booth and C. Price (Pergamon, Oxford, 1989), p. 311.
[3] L. Leuzzi and T. M. Nieuwenhuizen, Phys. Rev. E **64**, 011508 (2001).
[4] F. H. Stillinger and T. A. Weber, Phys. Rev. A **25**, 978 (1982).
[5] F. H. Stillinger and T. A. Weber, Science **225**, 983 (1984).
[6] F. H. Stillinger and T. A. Weber, Science **267**, 1935 (1995).
[7] S. Sastry, P. G. De Benedetti, and F. H. Stillinger, Nature (London) **393**, 554 (1998).
[8] A. Crisanti and F. Ritort, Physica A **280**, 155 (2000).
[9] A. Crisanti and F. Ritort, Europhys. Lett. **51**, 147 (2000).
[10] A. Crisanti and F. Ritort, Europhys. Lett. **52**, 640 (2000).
[11] A. Crisanti and H. J. Sommers, J. Phys. I **5**, 805 (1995).
[12] W. Kob, F. Sciortino, and P. Tartaglia, Europhys. Lett. **49**, 590 (1999).
[13] F. Sciortino, W. Kob, and P. Tartaglia, Phys. Rev. Lett. **83**, 3214 (1999).
[14] D. J. Thouless, P. W. Anderson, and R. G. Palmer, Philos. Mag. **35**, 593 (1977).
[15] Th. M. Nieuwenhuizen, e-print cond-mat/9911052.
[16] L. L. Bonilla, F. G. Padilla, G. Parisi, and F. Ritort, Phys. Rev. B **54**, 4170 (1996).
[17] L. L. Bonilla, F. G. Padilla, and F. Ritort, Physica A **250**, 315 (1998).
[18] Th. M. Nieuwenhuizen, Phys. Rev. Lett. **80**, 5580 (1998).
[19] R. J. Glauber, J. Math. Phys. **4**, 294 (1963).
[20] G. H. Fredrickson and H. C. Andersen, Phys. Rev. Lett. **53**, 1244 (1984).

[21] E. Follana and F. Ritort, Phys. Rev. B **54**, 930 (1996).
[22] W. Kob and H. C. Andersen, Phys. Rev. E **48**, 4364 (1993).
[23] J. Kurchan, L. Peliti, and M. Sellitto, Europhys. Lett. **39**, 365 (1997).
[24] H. Vogel, Phys. Z. **22**, 645 (1921); G. S. Fulcher, J. Am. Ceram. Soc. **8**, 339 (1925); G. Tammann and G. Hesse, Z. Anorg. Allg. Chem. **156**, 245 (1926).
[25] Th. M. Nieuwenhuizen, Phys. Rev. E **61**, 267 (2000).
[26] A. Garriga and F. Ritort, Eur. Phys. J. B **20**, 105 (2001).
[27] W. Kauzmann, Chem. Rev. **43**, 219 (1948).
[28] G. Biroli and R. Monasson, Europhys. Lett. **50**, 155 (2000).